PERGAMON

Available online at www.sciencedirect.com

SCIENCE DIRECT®

Computers and Structures 81 (2003) 2087–2098

Computers & Structures

www.elsevier.com/locate/compstruc

Development of computational software for analysis of curved girders under construction loads

Cem Topkaya, Eric B. Williamson *

Department of Civil Engineering, The University of Texas at Austin, Austin, TX 78712, USA

Received 14 October 2002; accepted 10 May 2003

Abstract

The analysis of horizontally curved, trapezoidal steel girders presents a variety of computational challenges. During the erection and construction stages before a concrete deck is available to form a closed section, these girders are weak in torsion and susceptible to warping. Considering the design of an entire bridge system, current design approaches favor the use of a grid analysis methodology. While the use of a grid analysis procedure offers the advantage of computational efficiency, it is unable to capture girder stresses and brace member forces with sufficient accuracy, particularly during the critical erection and construction stages. In this paper, we present an alternative analysis approach based on the finite element method. The developed software has been designed to be computationally efficient and easy to use for bridge designers.

Keywords: Bridge; Analysis; Finite elements; Construction; Curved girder; Software

1. Introduction

Curved, trapezoidal, steel box girders have been used extensively in recent years. A typical box girder system consists of one or more U-shaped steel girders that act compositely with a cast-in-place concrete deck through the use of welded shear studs (Fig. 1). The girders that typically comprise steel bridges are classified as thin-walled beams. Early research related to the theory of thin-walled beams is attributed to Timoshenko [1], Vlasov [2], and Dabrowski [3].

These researchers developed the fundamental equations for determining the stress/strain state over a cross-section for a given section geometry and loading. Direct solution of the governing equations for thin-walled curved girders is mathematically complex. Prior to the widespread use of computers, approximate methods, such as the M/R method [4], were most likely to be employed for design. Today, however, with the rapid improvement in computer technology, analyses are readily conducted by numerical simulation with the aid of various structural analysis software packages.

Aside from the behavior of a girder under service loads in the completed bridge, designers must also be concerned with the behavior of steel box girders during transport and construction. The design for construction loads is very important because stresses coming from construction loading can reach up to 60–70% of the total stresses on a cross-section [5]. Prior to hardening of the concrete deck, the box is an open section with limited torsional resistance (orders of magnitude less than when the section is closed). To prevent distortion of the cross-section during transport and erection, a lateral truss system is installed at a level close to the top flange in order to form what is often termed a "quasi-closed" cross-section. Determining the stress distribution over such a cross-section is quite difficult. Further complicating the situation is the fact that the bridge deck is typically not cast in one stage because the volume of

* Corresponding author. Tel.: +1-512-475-6175; fax: +1-512-471-7259.

E-mail address: ewilliamson@mail.utexas.edu (E.B. Williamson).

0045-7949/03/$ - see front matter © 2003 Elsevier Ltd. All rights reserved.
doi:10.1016/S0045-7949(03)00258-X

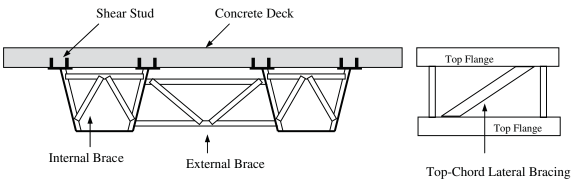

Fig. 1. A typical cross-section of a trapezoidal box girder system.

Fig. 2. Trapezoidal box girder failure during construction.

concrete is quite large. As a result, during the construction of a bridge, parts of the girders may become partially composite in sequential stages. Therefore, analysis for construction loading should take into account the partial composite action developing between the concrete deck and the quasi-closed cross-section.

Several options exist for numerical solutions to curved girder bridge analysis including grid analyses, the finite strip method, and the finite element method (FEM). The numerical approach that is routinely used by bridge designers is based on the grid method of analysis. The analysis of grids by the stiffness method is well established [6–8]. Grids are defined as structures in which all the loads are applied perpendicular to its plane. With grid analyses, members are normally assumed to be axially rigid, and bending about the weak axis is ignored. As a result of these assumptions, each node has three degrees of freedom (corresponding to transverse displacement, rotation about the major axis of the member, and twist around the member axis), and girders can be modeled as line elements. The primary strength of the grid analysis method is that it requires little computational effort to set up and solve, and it is fairly easy to use. Despite its computational efficiency, the grid method of analysis has some major drawbacks. Primarily, a large number of assumptions are built into this approach, and the analyst is somewhat limited by what they can model. An example of a common assumption is the use of the equivalent plate method [9] for establishing the torsional properties of a cross-section. With this method, the lattice of the top chord truss system is treated as a fictitious equivalent plate so that the girder can be modeled as having a closed cross-section. Following this approach, the stress distribution over the ‘‘closed’’ cross-section is more easily computed, and forces in the truss members can be determined once the stress distribution in the equivalent plate is known.

In order to be confident with the output from a grid analysis, the analyst must have a good understanding of the limitations of certain modeling assumptions. Thus, not only must the analyst understand, for example, the impact that different equivalent plate thicknesses can have on the computed results, he or she must also understand the implications of modeling an assemblage of members as a flat plate. Some recent failures of bracing members during construction (Fig. 2) demonstrate that engineers need more thorough information than that being provided by grid analyses. A similar issue that deserves consideration relates to the modeling of partial composite action within the framework of grid analyses. Because of the inherent limitations of this analysis approach, the partial composite action developing between pour stages is not easily modeled, and the variation of equivalent torsional properties must be assumed.

With the FEM, complex structures are divided into a large number of elements for which the behavior of each element is well defined. The response of a system is then computed by simply summing the effects of all the elements that comprise the model. Because the behavior of each element is known, the resulting system of equations, while perhaps very large, is readily solved. The finite element approach offers the advantages of being able to model the spatial configuration of a bridge and the ability to determine the stress and strain distribution at any location in a cross-section. Because the cross-section is modeled by a large number of finite elements, its actual shape is used for the analyses. As such, no assumptions related to thin-walled beam theory are needed. Furthermore, the top chord lateral bracing system can be modeled directly using beam or truss elements. The analyst need not resort to modeling the section as closed using the equivalent plate method. The only assumptions inherent in the FEM are related to the behavior of individual elements. The main drawback with the finite element approach is that accurate solutions require the solution of systems with many degrees of freedom, and extensive computer resources are needed under these circumstances. In addition, because most finite element software is written for general application, the development of a bridge's geometry for input into the analysis routine can be quite cumbersome and time consuming. For these reasons, the finite element approach has been used mostly in research settings, and it has seen limited use outside of universities.

Many of the problems engineers currently face when analyzing curved girders stem from the use of grid analyses. Aside from the cost of building models and the computational effort needed for a solution, the FEM offers tremendous potential to improve the way curved girders are currently designed. With the continuing advances in hardware capability, large-scale finite element analyses can now be conducted efficiently on personal computers. To take advantage of this capability, an easy-to-use finite element package (UTrAp) with a graphical user interface (GUI) was developed for the analysis of curved steel box girders under construction loads. The package consists of an analysis module, which was written in FORTRAN, and a GUI, which was written in Visual Basic. The program was developed for use on personal computers.

Rather than developing new software, commercially available finite element analysis software could have been used. With this approach, input files that account for various bridge geometries and loading scenarios could be developed using pre-processor commands that utilize the high-level input language found in most commercial software. The choice was made, however, to develop new software because this approach gives the greatest flexibility in designing the graphical input and output formats in a manner that is tailored to bridge engineers. In addition, it offers the advantage of not being reliant on commercial software that may not be used commonly by bridge designers. The following sections provide a detailed description of the capabilities and theoretical development of UTrAp.

2. Analysis module

The analysis module consists of a three-dimensional finite element program with pre- and post-processing capabilities. Input for the analysis module is provided by a text file that is created through use of the GUI. The module itself is capable of generating a finite element mesh, element connectivity data, and material properties based on the geometrical properties supplied through the GUI. The program also generates nodal loading based on the values given in the input file. After the pre-processing is completed, the program assembles the global stiffness matrix and solves the equilibrium equations to determine the displacements corresponding to a given analysis case. As a last step, the module post-processes the displacements in order to compute cross-sectional forces, stresses and brace member forces. The following sections document the formulation of the analysis module and discuss current capabilities and limitations.

3. Program capabilities

The analysis module is capable of analyzing curved, trapezoidal, steel box girders under construction loads. The program assumes a bridge geometry with a constant radius of curvature, and it considers only single and dual girder systems. The number of girders is limited to two because systems with more than two girders are not common in practice, and the analysis of such bridges with the FEM will require computer resources that surpass the capabilities of current personal computers. Nowadays, a typical PC used by an engineer has at least 256 MB memory and 1 GHz processor speed. Although not widely used currently, personal computers with up to 2 GB memory and 1.7 GHz processor speed are available. A typical twin girder system with the mesh adopted by this program requires about 700 MB of physical memory for in-core solution. Computer systems with less than this amount of memory require greater solution time because of the need to read and write to the hard drive during the solution procedure.

The analysis module allows the thickness of the plates to vary while the centerline dimensions of all components (e.g., web, top flange, etc.) are held constant. Internal, external and top lateral braces can be specified in the program, and supports can be placed at any location along the length of the bridge. There is no internal constraint on the number of braces, length of the bridge or number of supports. The program assumes linear response and is capable of handling multiple analysis cases in order to account for the number of concrete pours used in the construction sequence. The shear stud—concrete deck interaction at early concrete ages can also be included in the analyses. A study by Topkaya [10] revealed that composite action between the steel girders and concrete deck is achieved shortly after portions of the concrete deck have been placed. Therefore, in order to model accurately the behavior of a bridge during the construction process, it is essential to account for the development of strength and stiffness at the deck—girder interface that leads to portions of the bridge behaving in a partially composite manner. The program developed under this research is capable of modeling the partial composite action developing at early ages. For each concrete pour, the stiffness of the previously poured concrete deck(s) and that of the shear studs can be specified by the analyst. Recommendations for concrete and stud stiffness at early ages are given in Topkaya [10].

4. Input requirements

Geometric properties: The number of girders, radius of curvature, length of the bridge and cross-sectional dimensions are required input. Cross-sectional dimensions include depth of the web, width of the bottom flange, top flange width, width of the concrete deck and thickness of the concrete deck. In addition, the program requires the thickness of the web, bottom flange and top flange along the bridge length. There is no restriction on the number of different plate properties that a user can specify.

Supports: Support locations must be specified by the user. Locations are defined by the distance relative to a coordinate along the bridge's arc length. Supports are idealized to be either pinned or a roller. Actual properties of the support bearings are currently not considered in the program.

Braces: Locations, geometrical arrangement and areas of internal, external and top lateral braces must be specified.

Pour sequence: There can be several analyses performed that are independent of each other. The concrete deck can be divided into segments to account for the pouring sequence used during the construction of the bridge being modeled. The length of each segment must be provided as input. For each analysis, properties of the concrete deck can be varied. There are three properties associated with a deck segment including the concrete modulus, stud stiffness associated with a particular segment and the distributed load on the segment.

5. Algorithm of the analysis module

Program UTrAp uses nine-node shell elements as well as truss and spring elements to construct a finite element mesh. Steel plates and the concrete deck are modeled with shell elements. Braces and studs are modeled with truss and spring elements, respectively. The following paragraphs present the details of the program algorithm.

5.1. Node locations and element connectivity

The program automatically forms the node locations and element connectivity based upon the geometric properties of the bridge specified by the user through the GUI. A constant mesh density is used for all bridges. The webs and bottom flanges of the girders are modeled with four shell elements, and two elements are used for the top flanges. The concrete deck is modeled with 10 and 20 shell elements for single and dual girder systems, respectively. Previous work on curved trapezoidal girders [11] revealed that this mesh density provides suitable accuracy for the cross-sectional dimensions typically used in practice. Along the length of the bridge, each element is 0.61 m (2 ft) long. This mesh density assures elements with aspect ratios less than two for most practical cases. According to the geometrical dimensions and radius of curvature, the program forms the locations of the nodes. For each node, three mutually orthogonal unit vectors $(\boldsymbol{V}_1, \boldsymbol{V}_2, \boldsymbol{V}_3)$ are created. These unit vectors are used in defining the shell element geometry. Fig. 3 shows the nodes and unit vectors on a single girder system. Unit vectors are formed in such a way that $\boldsymbol{V}_3$ points in the direction through the thickness of the shell element and $\boldsymbol{V}_2$ is tangent to the arc along the bridge length. The vector $\boldsymbol{V}_1$ is formed such that it is orthogonal to both $\boldsymbol{V}_2$ and $\boldsymbol{V}_3$.

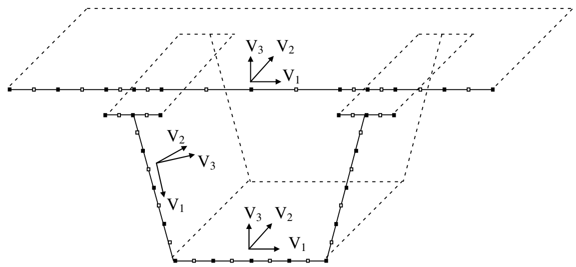

Fig. 3. Node locations and unit vectors.

5.2. Modeling of the physical system

There are several modeling techniques presented in the literature for analyzing the steel girder—concrete deck interaction. One proposed method is to model the steel section with shell elements and the concrete deck with brick elements [12] (Fig. 4). Spring elements are placed at the interface to model the shear studs. This type of modeling approach produces a very large number of degrees of freedom because, in order to capture the flexural response of the deck with sufficient accuracy, a large number of brick elements must be used.

In another technique, both the steel cross-section and the concrete deck are modeled with shell elements [13,14]. The steel and concrete sections are linked together with connector (beam) elements (Fig. 4). The length of the connector elements has to be chosen by the analyst to properly model the offset between the neutral axis of the top flange of the girders and that of the deck. This approach is the most commonly reported technique presented in the literature. It is important to point out that this modeling methodology is prone to numerical problems because of the use of very short connector elements. Not only is the ratio of the length to the cross-

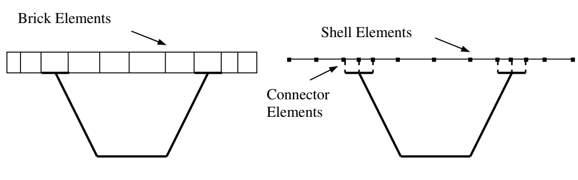

Fig. 4. Different modeling techniques for deck-flange interface.

sectional dimensions inconsistent with standard beam element formulations, small displacements can lead to large rotations of the connector element axis if the element is too short.

In the software developed for the current research, another approach is used to model the cross-section which addresses both problems mentioned above. Two types of shell elements were used in modeling a given cross-section. In a shell element formulation, the three-dimensional domain is represented by a surface. The selection of the representative surface depends on the particular formulation being considered. For the linear formulation used in the program, any surface along the thickness can be considered as a reference surface. The two types of shell elements used in the program are similar in formulation but differ in their reference surface definitions. For steel sections, the reference surface is considered to be the middle surface, while for the concrete deck, the bottom surface is used as the reference surface (Fig. 5). The steel sections and the concrete deck are connected together by spring elements that represent the stud connectors. This modeling technique requires fewer degrees of freedom for accurate results when compared with the brick model. In addition, it properly models the interface behavior by eliminating the link elements and including the girder offset by using the bottom shell surface of the concrete deck elements as the reference surface.

Internal, external and top lateral braces are modeled with truss elements. Initially, beam elements were also considered, but the analysis results showed that the flexural response of the brace members could be safely ignored. The program calculates the nodal connectivity of the brace elements from the supplied location values. Currently, only one type of internal brace and one type of external brace is handled in the program (Fig. 1). The ones included are the typical types used in practice. Other geometrical arrangements for the braces can be added to the software as needed.

Linear spring elements are used to model the shear studs. For each top flange, three nodes are connected to the concrete deck. The connection is achieved by spring elements in all three global directions. Springs are placed every 0.3 m (1 ft) along the bridge length even if studs are not physically present. The stiffness properties of each spring element are modified according to the physical distribution of studs in a particular region. For each spring element there is a corresponding stiffness modification factor. The modification factor is calculated by dividing the stud spacing value by 0.3 m (12 in.). If there are less than three studs per flange, very low modification factors (10^{-8}) are assigned to the studs in the finite element model which correspond to locations where shear connectors are physically not present. In the case where the number of studs per flange is greater than three, the modification factor is computed by taking the number of studs per flange and dividing by three.

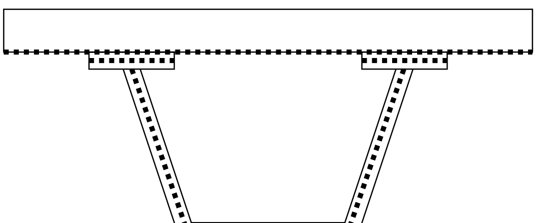

Fig. 5. Reference surfaces for shell elements.

For the cases where there is no composite action, a user may specify zero concrete or stud stiffness. The presence of zero stiffness elements, however, will lead to an ill-conditioned structural stiffness matrix. In order to overcome this numerical problem, low stiffness values (7.0×10^{-5} MPa (10^{-5} ksi) and 1.5×10^{-4} kN/mm (10^{-5} k/in.)) are assigned to the concrete deck and shear studs, respectively, by the analysis module.

Even if the construction loads act through the shear center of the cross-section, internal torsional forces develop along the length of the bridge due to the horizontal curvature of the bridge centerline. The highest torsional forces generally occur at the support locations. In practice, diaphragms in the form of thick plates are placed at the support locations to reduce stresses caused by high torsional forces. Diaphragms form a solid cross-section with very high torsional and distortional stiffness. The program internally assembles a very stiff truss system at the support locations to simulate the effects of the steel diaphragm. These elements are placed at locations where a support is specified. The stiff truss system prevents distortion of the cross-section by restraining the relative movements of the edges. Thus, the behavior of the girder cross-section is accurately modeled, and no additional degrees of freedom are needed to incorporate the effects of the diaphragms.

5.3. Assembly of the global stiffness matrix

Based on the shell element connectivity and boundary conditions, degrees of freedom are assigned to nodes throughout the structure. After the degrees of freedom have been determined, the global stiffness matrix is assembled. Because internal and external braces have nodes that are not shared with shell elements, a condensation technique is used to eliminate the degrees of freedom associated with those nodes. First, the truss elements are assembled together to form a “superelement”. Second, the degrees of freedom which are not shared with the steel girder are condensed out. During the kinematic condensation, numerical singularities may occur due to round-off errors as well as a lack of stiffness for motion perpendicular to the plane of the three-dimensional truss. In order to alleviate this problem, rather than resorting to a nonlinear element formulation that is capable of treating out-of-plane deformations, very flexible springs in all three global directions are placed at the nodes where four of the truss members meet. This approach was found to be computationally efficient while still providing for accurate calculations of the truss member forces. After assembling the springs, the condensation is carried out. The following sections summarize the formulation of the element stiffness matrices used in the program.

5.4. Shell element formulation

A nine-node, isoparametric shell element (degenerated brick) originally developed by Ahmad et al. [15] was implemented in the program (Fig. 6). At each node, a unit vector $\boldsymbol{V}_3$ extends through the thickness of the element. Unit vectors $\boldsymbol{V}_1$ and $\boldsymbol{V}_2$, along with $\boldsymbol{V}_3$, form a set of mutually orthogonal vectors that help define the shell geometry. The unit vectors undergo rigid body motion during the deformation of the element. The element is mapped into material coordinates (ξ, η, ζ) where ξ, η are the two coordinates in the reference plane and the ζ coordinate is oriented through the thickness of the shell. The geometry $\boldsymbol{x}$ throughout the element is interpolated as follows:

$$\boldsymbol{x}(\xi,\eta,\zeta) = \sum_{i=1}^{9}\left[\left(\boldsymbol{x}_i + \zeta\frac{h}{2}\boldsymbol{V}_3\right)N_i(\xi,\eta)\right] \tag{1}$$

where h is the thickness of the shell and $N_i(\xi,\eta)$ are the Lagrangian shape functions given explicitly in Bathe [16].

The displacement field is defined by the three global displacement (u, v, w) and two rotational (α, β) degrees of freedom. Rotation around $\boldsymbol{V}_3$, often termed the "drilling" degree of freedom, is not included. In order to define the rotation axes for α and β, a right-handed triplet of mutually orthogonal unit vectors $(\boldsymbol{V}_1, \boldsymbol{V}_2, \boldsymbol{V}_3)$ are used. Rotations α and β are the rotations about the $\boldsymbol{V}_1$ and $\boldsymbol{V}_2$ (Fig. 6) axes, respectively. The displacement field $\boldsymbol{u}$ is interpolated as follows:

$$\boldsymbol{u}(\xi,\eta,\zeta) = \sum_{i=1}^{9}\left[\left(\boldsymbol{u}_i + \zeta\frac{h}{2}(-\alpha_i\boldsymbol{V}_2 + \beta_i\boldsymbol{V}_1)\right)N_i(\xi,\eta)\right] \tag{2}$$

where $\boldsymbol{u}_i$ is the vector of Cartesian components of the reference surface displacement at node i.

The element formulation includes the basic shell assumption that the stress normal to any lamina ($\zeta =$ constant) is zero. This assumption implies that at any point in the domain, a local rigidity matrix, similar to the one used in two-dimensional plane stress analysis, must be used. For analysis of an assemblage of shell elements, this local rigidity matrix has to be transformed into global coordinates. For transformation purposes, the local orthogonal coordinate axes consisting of unit vectors $\boldsymbol{t}_1$, $\boldsymbol{t}_2$, $\boldsymbol{t}_3$ need to be formed, where $\boldsymbol{t}_3$ is the vector normal to the shell surface at the point of consideration (integration point). The orthogonal local axes are formed according to Algorithm 1:

Algorithm 1

1. At the point of consideration:

$$\boldsymbol{t}_1 = \frac{\partial}{\partial\xi}\boldsymbol{x} \quad \boldsymbol{t}_2 = \frac{\partial}{\partial\eta}\boldsymbol{x}$$

2. Form unit vectors:

$$\boldsymbol{t}_1 = \frac{\boldsymbol{t}_1}{|\boldsymbol{t}_1|} \quad \boldsymbol{t}_2 = \frac{\boldsymbol{t}_2}{|\boldsymbol{t}_2|}$$

3. Calculate the normal vector $\boldsymbol{t}_3$:

$$\boldsymbol{t}_3 = \boldsymbol{t}_1 \times \boldsymbol{t}_2$$

4. Re-orient the $\boldsymbol{t}_2$ vector:

$$\boldsymbol{t}_2 = \boldsymbol{t}_3 \times \boldsymbol{t}_1$$

By making use of the direction cosines of the orthonormal local axes, a transformation matrix $\boldsymbol{R}$ is formed. The global rigidity matrix is calculated as follows:

$$\boldsymbol{D} = \boldsymbol{R}^{\mathrm{T}}\boldsymbol{D}^{\mathrm{local}}\boldsymbol{R} \tag{3}$$

where $\boldsymbol{D}^{\mathrm{local}}$ is the local rigidity matrix.

$$\boldsymbol{D}^{\mathrm{local}} = \frac{E}{1-\upsilon^2}\begin{bmatrix} 1 & \upsilon & 0 & 0 & 0 & 0 \\ \upsilon & 1 & 0 & 0 & 0 & 0 \\ 0 & 0 & 0 & 0 & 0 & 0 \\ 0 & 0 & 0 & \frac{1-\upsilon}{2} & 0 & 0 \\ 0 & 0 & 0 & 0 & \frac{1-\upsilon}{2} & 0 \\ 0 & 0 & 0 & 0 & 0 & \frac{1-\upsilon}{2} \end{bmatrix} \tag{4}$$

where E is the modulus of elasticity and υ is the Poisson's ratio.

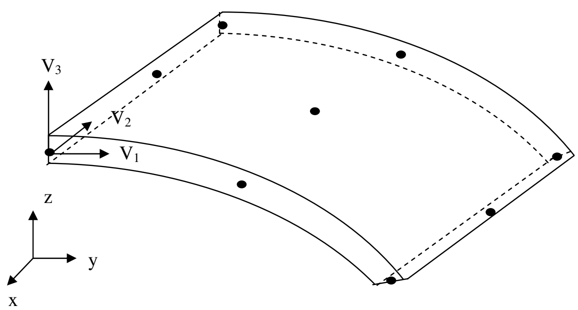

Fig. 6. Nine-node shell element.

$$
\boldsymbol{R} = \begin{bmatrix}
\boldsymbol{t}_{1x}^2 & \boldsymbol{t}_{1y}^2 & \boldsymbol{t}_{1z}^2 & \boldsymbol{t}_{1x}\boldsymbol{t}_{1y} & \boldsymbol{t}_{1x}\boldsymbol{t}_{1z} & \boldsymbol{t}_{1y}\boldsymbol{t}_{1z} \\
\boldsymbol{t}_{2x}^2 & \boldsymbol{t}_{2y}^2 & \boldsymbol{t}_{2z}^2 & \boldsymbol{t}_{2x}\boldsymbol{t}_{2y} & \boldsymbol{t}_{2x}\boldsymbol{t}_{2z} & \boldsymbol{t}_{2y}\boldsymbol{t}_{2z} \\
\boldsymbol{t}_{3x}^2 & \boldsymbol{t}_{3y}^2 & \boldsymbol{t}_{3z}^2 & \boldsymbol{t}_{3x}\boldsymbol{t}_{3y} & \boldsymbol{t}_{3x}\boldsymbol{t}_{3z} & \boldsymbol{t}_{3y}\boldsymbol{t}_{3z} \\
2\boldsymbol{t}_{1x}\boldsymbol{t}_{2x} & 2\boldsymbol{t}_{1y}\boldsymbol{t}_{2y} & 2\boldsymbol{t}_{1z}\boldsymbol{t}_{2z} & \boldsymbol{t}_{1x}\boldsymbol{t}_{2y} + \boldsymbol{t}_{1y}\boldsymbol{t}_{2x} & \boldsymbol{t}_{1x}\boldsymbol{t}_{2z} + \boldsymbol{t}_{1z}\boldsymbol{t}_{2x} & \boldsymbol{t}_{1y}\boldsymbol{t}_{2z} + \boldsymbol{t}_{1z}\boldsymbol{t}_{2y} \\
2\boldsymbol{t}_{1x}\boldsymbol{t}_{3x} & 2\boldsymbol{t}_{1y}\boldsymbol{t}_{3y} & 2\boldsymbol{t}_{1z}\boldsymbol{t}_{3z} & \boldsymbol{t}_{1x}\boldsymbol{t}_{3y} + \boldsymbol{t}_{1y}\boldsymbol{t}_{3x} & \boldsymbol{t}_{1x}\boldsymbol{t}_{3z} + \boldsymbol{t}_{1z}\boldsymbol{t}_{3x} & \boldsymbol{t}_{1y}\boldsymbol{t}_{3z} + \boldsymbol{t}_{1z}\boldsymbol{t}_{3y} \\
2\boldsymbol{t}_{2x}\boldsymbol{t}_{3x} & 2\boldsymbol{t}_{2y}\boldsymbol{t}_{3y} & 2\boldsymbol{t}_{2z}\boldsymbol{t}_{3z} & \boldsymbol{t}_{2x}\boldsymbol{t}_{3y} + \boldsymbol{t}_{2y}\boldsymbol{t}_{3x} & \boldsymbol{t}_{2x}\boldsymbol{t}_{3z} + \boldsymbol{t}_{2z}\boldsymbol{t}_{3x} & \boldsymbol{t}_{2y}\boldsymbol{t}_{3z} + \boldsymbol{t}_{2z}\boldsymbol{t}_{3y}
\end{bmatrix} \tag{5}
$$

where $\boldsymbol{t}_{ix}$, $\boldsymbol{t}_{iy}$, $\boldsymbol{t}_{iz}$ are the direction cosines of vector $\boldsymbol{t}_i$ with respect to global x, y, z axes, respectively.

The stiffness matrix is calculated as:

$$
\boldsymbol{K} = \int_\Omega \boldsymbol{B}^{\mathrm{T}}\boldsymbol{D}\boldsymbol{B}\,\mathrm{d}\Omega \tag{6}
$$

where Ω is defined as the domain of the element.

In UTrAp, computation of the stiffness matrix in Eq. (6) is achieved using full integration—3 Gauss integration points in each ξ, η direction and 2 integration points in the ζ direction. Full integration was used to alleviate the problems associated with spurious modes that can result when using reduced integration, and can lead to unstable or very inaccurate solutions.

Future research will focus on the use of reduced integration for computing the response of multiple girder systems. In addition, comparative studies for evaluating the solution accuracy for both reduced integration and full integration will be carried out. While full integration may lead to a solution that is too stiff, reduced integration, as discussed above, can also lead to inaccurate solutions. Thus, future work will endeavor to determine which approach provides acceptably accurate solutions with the least amount of required computational effort.

5.5. Truss and spring element formulations

A standard three-dimensional, two-node linear truss element and a standard two-node, three-dimensional translational spring element is implemented in the program. Details of the formulations can be found in McGuire et al. [17].

5.6. Solution capability

Large-scale, finite element analyses produce a system of linear equations which requires extensive computer resources to be solved. Until recently, most of these analyses were performed on UNIX workstations. With advances in hardware technology, large-scale systems can be handled on personal computers. Because bridges are long and thin structures, the mesh adopted (Fig. 7) to represent the physical model produces a global stiffness matrix that is sparse in nature. In sparse systems, many of the entries in the stiffness matrix are zero. While standard techniques can be used to solve the resulting system of equations, much greater efficiency can be realized if advantage is taken of the sparse nature of the stiffness matrix. Two types of sparse solvers, either direct or iterative, can be used to compute a solution. Iterative solvers were found to create numerical problems in models involving shell elements [18]. Therefore, in the program developed for this research, a direct sparse solver was chosen for the solution of the system of linear equations. A sparse solver developed by Compaq, which is a part of the Compaq Extended Math Library (CXML), has been adapted to the program. The solver is supplied as a library file by the Compaq Visual

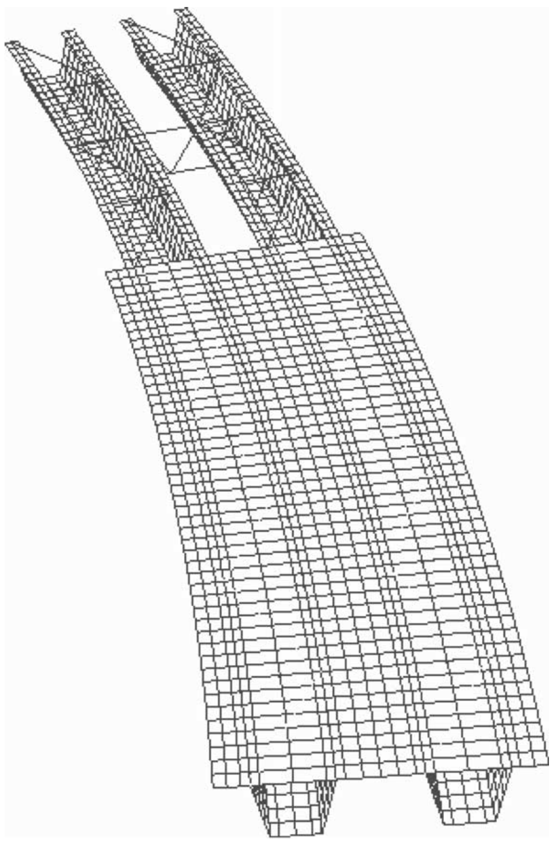

Fig. 7. Portion of a finite element model.

Fortran 6.5 compiler and can be compiled with the finite element program. Only the nonzero entries of the upper triangular half of the matrix need to be stored. In addition, two vectors, which are used to define the locations of the nonzero entries, are required by the solver. Based on the information of nonzero entries and their locations, the solver is capable of reordering and factoring the stiffness matrix and solving for displacements. The solver dynamically allocates all the arrays required during the solution process. It is capable of performing operations using the virtual memory whenever available physical memory is not sufficient.

The nonzero terms in the global stiffness matrix are located in rows and columns which correspond to the degrees of freedom that are connected to each other. Before the global stiffness matrix is assembled, the two position vectors that keep track of the locations of the nonzero terms have to be formed. A subroutine was developed for this purpose. The subroutine accepts the nodal connectivity information as input. For each degree of freedom, all associated degrees of freedom are found. This information is then used to form the two position vectors.

At the initial stages of the program development, several other solvers were considered for adoption into the analysis module. The NASA Vector Sparse Solver [19], Y12maf sparse solver [20], a frontal solver developed at the University of Texas at Austin, and the CXML sparse solver were compared. The CXML solver was found to be the most efficient in terms of memory usage and speed of solution on the single processor personal computers available.

5.7. Post-processing capability

The program is capable of generating output useful to designers based on the displacements computed from the analyses. Output obtained from post-processing is written to text files which can be read through use of the GUI. The program outputs vertical deflection of the girder centerline as well as the cross-sectional rotation along the length of the bridge. In addition, the program calculates axial forces for all top lateral, internal and external braces. Cross-sectional stresses and forces are calculated at every 0.61 m (2 ft) along the bridge length because elements have a length of 0.61 m. For each cross-section, stresses at the center of the top surface for each element are calculated. Therefore, for each cross-section, shear and normal stresses are printed out at 26 and 52 locations for single and dual girder systems, respectively. These stress components are given in the local directions (i.e., normal and perpendicular to the cross-section). In order to compute these stresses, strains in global directions must be transformed to quantities in local directions. Strains in local coordinates are further multiplied by the rigidity matrix so that the assumption of stress normal to any lamina be zero is maintained. In addition to stresses, cross-sectional shear, moment and torsion are calculated every 0.61 m (2 ft) along the length of the bridge. For any cross-section, the nodal internal forces and moments are computed for all the nodes that lie on that cross-section. These forces and moments are transformed from global coordinates to local coordinates. Finally, the transformed forces and moments for all elements are combined to compute the total internal stress resultants on the cross-section.

6. Graphical user interface

The GUI was designed to provide an environment in which a user can easily enter the required input data. In addition, the GUI has the capability of displaying both the numerical and graphical output of the analysis results. Fig. 8 shows the main form of the interface, and viewing from top to bottom, it displays the plate thickness properties, pour sequence and the plan view of the bridge. The GUI is written in Visual Basic and has the following menus and graphics capabilities.

File menu: This menu consists of submenus and is used for data management. A user can either start a new project (a new project description) or continue with an existing project. Any changes made to a new or existing project can be saved with the ‘‘Save Project’’ option.

Geometry menu: This menu brings the ‘‘Geometric Properties’’ form to the screen (Fig. 9). Information on the number of girders, radius of curvature, length of bridge, girder offset and cross-sectional dimensions are supplied by making use of this form.

Plate properties menu: This menu brings the ‘‘Plate Properties’’ form to the screen. This form has three folders for entering web thickness, bottom flange

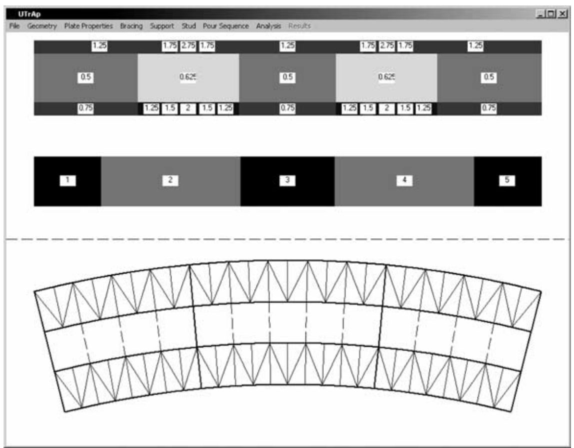

Fig. 8. The graphical user interface.

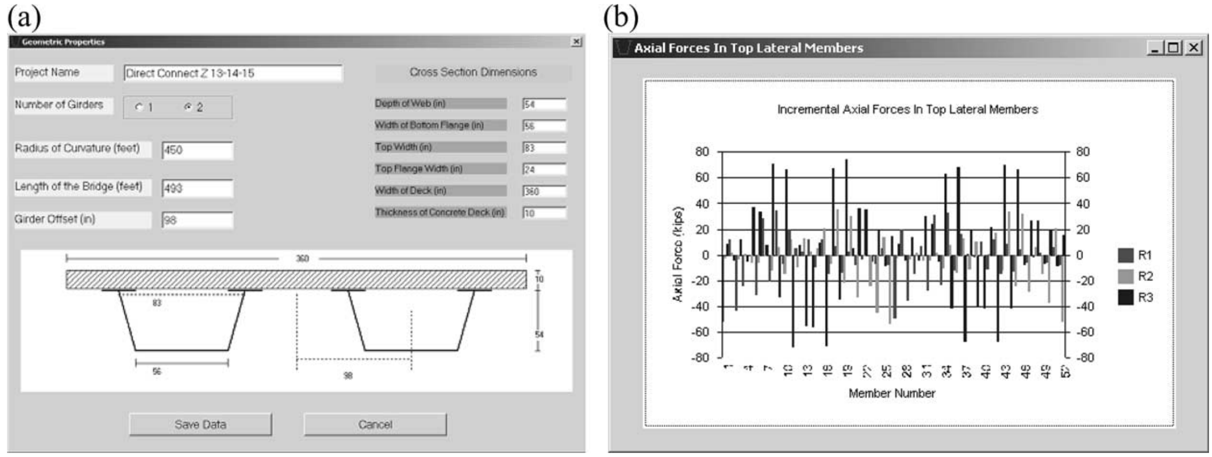

Fig. 9. Views from the graphical user interface: (a) geometric properties (input) and (b) axial forces in top lateral members (output).

thickness, and top flange thickness properties as a function of the position along the length of the bridge.

Bracing menu: This menu brings the "Bracing Properties" form to the screen. This form has three folders for entering internal brace, external brace, and top lateral brace information. For internal and external braces, location of the brace, its type and cross-sectional area of its members need to be specified. For top lateral braces, start and end locations, type and cross-sectional area information need to be supplied. Each folder has buttons to assign the same type and cross-sectional area to all the brace members. In addition, buttons are provided for entering equally-spaced braces between two user-specified locations.

Support menu: This menu brings the "Support Locations" form to the screen. In this form, the locations of the supports are entered by the user.

Stud menu: This menu brings the "Stud Properties" form to the screen. In this form, the spacing of the shear studs and the number of studs per flange along the length of the girder need to be supplied.

Pour sequence menu: This menu brings the "Pour Sequence" form to the screen. With this form, tabulated data related to the pour sequence can be supplied. Several different analysis cases can be specified, and the concrete deck can be divided into segments (Fig. 8). The length of each segment needs to be entered. For each analysis case, concrete modulus, stiffness and loading information for every deck segment needs to be provided.

Analysis menu: This menu executes the analysis module. Before starting the analyses, a text input file, which is read by the analysis module, is prepared based on the information supplied in the GUI. It should be noted that extensive error checking is carried out during pre-processing and prior to execution of the analysis routine. Thus, consistency in the structural layout and arrangement is verified before the finite element analyses are initiated.

Results menu: This menu has eight submenus. The submenus are used to visualize the analysis results. Vertical deflection and cross-sectional rotation of the bridge, brace member forces, cross-sectional stresses and forces can be tabulated or displayed graphically (Fig. 9). Detailed procedures for using the software can be found in Topkaya [10].

7. Verification of the program with published solutions

Results from the developed software were compared with published solutions. Researchers Fan and Helwig [21] developed a simplified method for predicting the top lateral brace member forces in curved box girders. The method proposed by Fan and Helwig [21] was compared against an independent finite element analysis performed using a commercially available, general-purpose program (ANSYS). The predictions of the simplified method were in excellent agreement with the finite element analyses. In this section, the published finite element analysis results are compared with the results obtained from UTrAp. The bridge analyzed by Fan and Helwig [21] was a three-span, single girder system having a radius of 291 m (954.9 ft) and a length of 195 m (640 ft). Details of the bridge are given in Fig. 10. Internal braces were located at every 3 m (10 ft), and an X-type top lateral system between internal brace points was utilized. The top lateral brace members were WT 6×13 sections, while the internal brace elements were L 4×4× 5/16 sections. The bridge was analyzed under a uniform load of 48.2 kN/m (3.3 k/ft). A constant top flange width of 35.6 cm (14 in.) was assumed.

The top lateral members were divided into two groups (X1 and X2) according to their orientation. Force levels

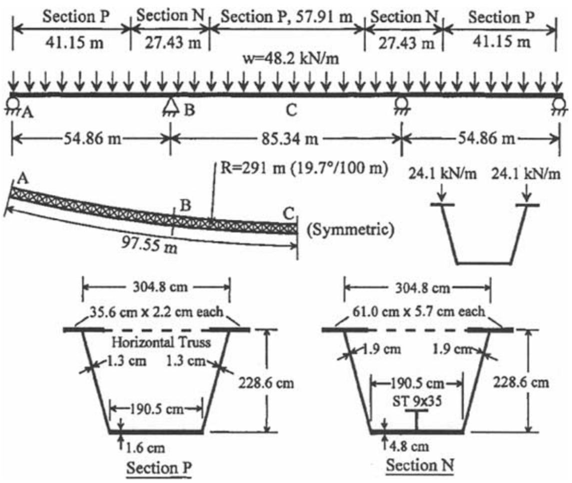

Fig. 10. Layout and cross-sectional dimensions of the bridge (appears as Fig. 6 in Fan and Helwig [21], reproduced with the permission of ASCE).

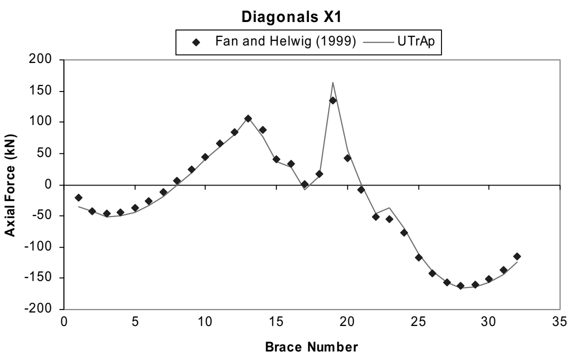

Fig. 11. Comparison of published and UTrAp results for X1 diagonals.

for these top lateral members obtained from finite element analysis were presented by Fan and Helwig [21]. These force levels are compared with the predictions from UTrAp in Figs. 11 and 12. These figures clearly demonstrate that the developed software is capable of

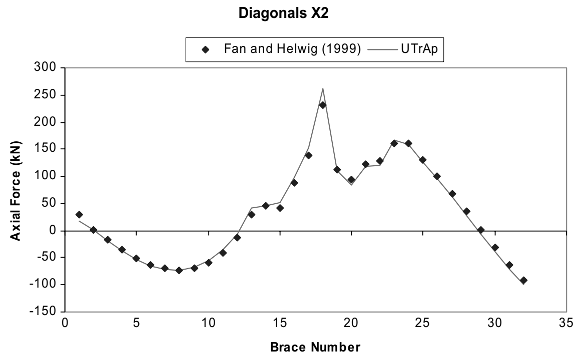

Fig. 12. Comparison of published and UTrAp results for X2 diagonals.

producing results similar to published solutions. In the next section, the program will be compared with experimental findings.

8. Verification of the program with experimental findings

The research presented herein was part of an overall program evaluating the behavior of curved, steel, trapezoidal box girders. Aside from the development of the software described in this paper, one component of the project required monitoring of two curved bridges during construction. Forces in top lateral brace members and cross-sectional stresses were measured during the course of casting the concrete deck in several segments. The measured forces and stresses were compared with the predictions obtained using the developed software. In this section, a representative comparison between the measured and predicted values is given.

One of the bridges that was monitored as a part of the research program was called "Connect K" (Fig. 13). It is a three-span, dual girder bridge with two side spans of 51 m (168 ft) and a middle span of 74 m (242 ft). The centerline radius of the bridge is 175 m (573 ft). The concrete deck was cast in five segments. Eight top lateral members and four cross-sections were monitored during

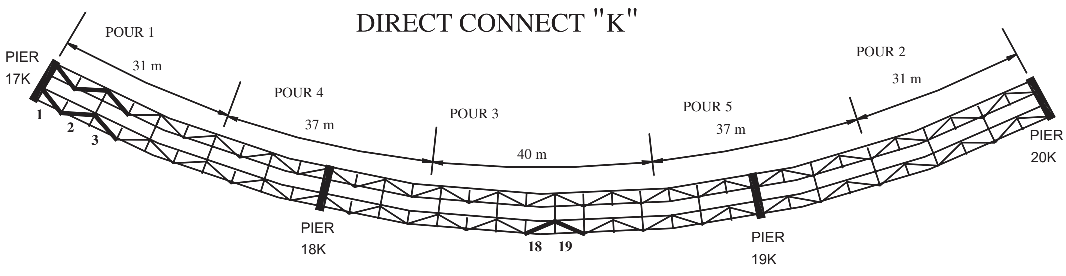

Fig. 13. Plan view of instrumented bridge.

construction. Six of the instrumented top laterals were located in the first three panels at Pier 17 K (Fig. 13). The remaining two instrumented laterals were located at panels 18 and 19 of the outer girder (Fig. 13). Cross-sectional stresses were monitored at the top and bottom flanges of four girder cross-sections. Two of the instrumented cross-sections were located in the middle of panels 2 and 3. For these locations, both the inner and outer girders were monitored. The remaining two instrumented cross-sections were located in the middle of panels 18 and 19. For these locations, only the outer girder was monitored.

In constructing the bridge, the first pour had a length of 31 m (100 ft) and was at the 17 K end of the bridge (Fig. 13). Figs. 14 and 15 show the changes in the top lateral forces and cross-sectional stresses for pour 1 along with the analytical predictions.

In Fig. 15, the following nomenclature is used: Out = outer girder, In = inner girder, T = top flange, and B = bottom flange. Therefore, Out 3B corresponds to the change in stress at the bottom flange of the outer girder in the middle of panel 3.

A comparison to measured field data shows that the developed program provides an accurate characterization of the girder response under construction loads. Current research is working to further improve the correspondence between the UTrAp predictions and the results obtained from field data. A more in-depth discussion of the comparisons between the measured response and the predicted response can be found in Topkaya [10].

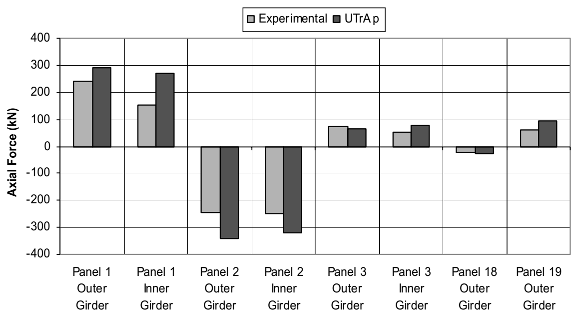

Fig. 14. Change in axial force levels due to pour 1.

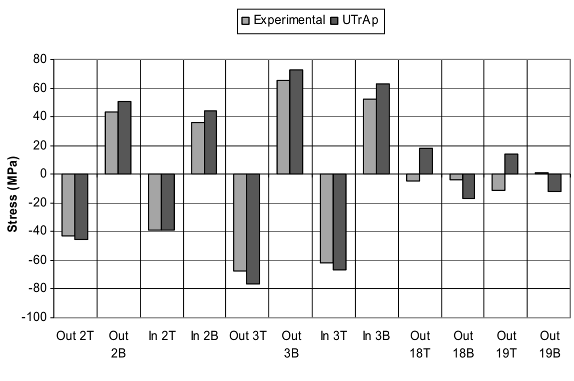

Fig. 15. Change in cross-sectional stresses due to pour 1.

9. Conclusions

The development of an easy-to-use computational software package for analysis of curved, steel, trapezoidal box girders under construction loads was presented. The computer program consists of an analysis module and a GUI. The analysis module is capable of performing a full three-dimensional finite element analysis for these structural systems and has pre- and post-processing capabilities. The use of current analytical tools in the design of curved girders has resulted in designs of internal brace members that are not conservative. Improved accuracy in computing girder stresses and brace forces are expected with the use of the developed software, and time and effort needed to obtain the solution from UTrAp is only slightly greater than traditional analyses with the grid method. The following can be concluded from this study:

- Current analytical tools available to designers for curved girder analysis were found to be inadequate. A computer program capable of performing three-dimensional finite element analyses is essential for this purpose.
- Advances in computer technology enable large-scale finite element analyses to be performed on personal computers.
- With the use of proper pre- and post-processing techniques, finite element analyses of curved girders can be made much more designer friendly. The developed computer program requires minimal knowledge of the theoretical aspects of the FEM.
- The use of shell elements, where the bottom surface is the reference surface, for modeling the bridge deck was proposed as an alternative to current modeling techniques. The use of this technique eliminates the use of link elements and reduces the degrees of freedom by a significant amount over models with brick elements. Thus, the method used in this research has the advantage of greater accuracy and fewer degrees of freedom when compared to traditional modeling approaches.
- Sparse solvers were found to be effective for this kind of analysis problem.

Acknowledgements

This research was part of a larger research project supported by a contract from the Texas Department of

Transportation (TxDOT Project no. 1898). The conclusions drawn in this paper are the opinions of the authors and do not necessarily reflect the opinions of the sponsor. In addition, the writers would like to extend special thanks to Prof. Joseph A. Yura at the University of Texas for his guidance and help.

References

[1] Timoshenko SP, Gere JM. Theory of elastic stability. 2nd ed. New York: McGraw-Hill; 1961.
[2] Vlasov VZ. Thin-walled elastic beams. 2nd ed. Washington, DC: National Science Foundation; 1961.
[3] Dabrowski R. Curved thin-walled girders. London: Cement and Concrete Association; 1968.
[4] Tung DHH, Fountain RS. Approximate torsional analysis of curved box girders by the M/R method. Eng J AISC 1970;7(3):65–74.
[5] Holt J. TxDOT Design Engineer, Personal Correspondence, 2001.
[6] Razaqpur AG, Li H. Thin-walled multicell box-girder for finite element. ASCE J Struct Eng 1991;117(10):2953–71.
[7] Zhang SH, Lyons LPR. A thin-walled box beam finite element for curved bridge analysis. Comput Struct 1984;18(6):1035–46.
[8] Fu CC, Hsu YT. The development of an improved curvilinear thin-walled Vlasov element. Comput Struct 1995;54(1):147–59.
[9] Kollbrunner CF, Basler K. Torsion in structures—an engineering approach. New York: Springer-Verlag; 1969.
[10] Topkaya C. Behavior of curved steel trapezoidal box girders during construction. PhD Dissertation, University of Texas at Austin, Austin, TX, 2002.
[11] Fan Z. Field and computational studies of steel trapezoidal box girder bridges. PhD Dissertation, University of Houston, 1999.
[12] Tarhini KM, Frederick GR. Wheel load distribution in I-girder highway bridges. ASCE J Struct Eng 1992;118(5): 1285–94.
[13] Brockenbrough RL. Distribution factors for curved I-girder bridges. ASCE J Struct Eng 1986;112(10):2200–15.
[14] Tabsh SW, Sahajwani K. Approximate analysis of irregular slab-on-girder bridges. ASCE J Bridge Eng 1997;2(1): 11–7.
[15] Ahmad S, Irons BM, Zienkiewicz OC. Analysis of thick and thin shell structures by curved finite elements. Int J Numer Meth Eng 1970;2:419–51.
[16] Bathe KJ. Finite element procedures in engineering analysis. Englewood Cliffs, NJ: Prentice-Hall, Inc.; 1982.
[17] McGuire W, Gallagher RH, Ziemian RD. Matrix structural analysis. 2nd ed. New York: John Wiley & Sons Inc.; 2000.
[18] Gullerud AS, Koppenhoefer KC, Roy A, RoyChowdhury S, Dodds RH. WARP3D-Release 13.12. 3-D dynamic nonlinear fracture analysis of solids using parallel computers and workstations. Research Report, Structural Research Series No. 607, University of Illinois at Urbana-Champaign, 2001.
[19] Storaasli OO. Performance of NASA equation solvers on computational mechanics applications. 37th AIAA/ASME/ASCE/AHS/ASC Structures, Structural Dynamics and Materials Conference, Paper No. 96-1505, Salt Lake City, UT, 1996, p. 1680–5.
[20] Zlatev Z, Wasniewski J, Schaumburg K. Y12M: solution of large and sparse systems of linear algebraic equations. Lecture Notes in Computer Science. Berlin, Heidelberg: Springer-Verlag; 1981.
[21] Fan Z, Helwig TA. Behavior of steel box girders with top flange bracing. ASCE J Struct Eng 1999;125(8):829–37.